Proceedings of the EuroGNC 2013, 2nd CEAS Specialist Conference on
Guidance, Navigation & Control, Delft University of Technology, Delft,
The Netherlands, April 10-12, 2013

Spacecraft Attitude Control based on Magnetometers and Gyros

Marco Bergamasco and Marco Lovera

Abstract The problem of designing attitude control laws for a Low Earth Orbit (LEO) satellite on the basis of static feedback from a triaxial magnetometer and a set of high precision gyros is considered and an approach based on optimal static output feedback for linear time-periodic system is presented. Simulation results are used to demonstrate the feasibility of the proposed strategy and to evaluate its performance in a realistic setting.

1 Introduction

Angular rate sensors are frequently used in space missions to provide either an accurate alternative to pseudo-derivatives of attitude measurements in the implementation of derivative feedback or as a source of accurate attitude measurements in rate integration mode, for, e.g., high accuracy attitude manoeuvres (see, e.g., [13, 17]). Unfortunately it is well known that the main issue associated with rate gyro feedback is the presence of bias and drift (see, e.g., [4]), which make such sensors poorly reliable over long time spans and introduce the need for on-line estimation of calibration parameters. The availability of new generation angular rate sensors with significantly improved characteristics in terms of bias and bias stability (see, e.g., [3, 11]), however, might lead to a very different scenario as far as attitude control systems (ACS) design is concerned, since they would make it possible to design and implement control laws with highly accurate derivative action with limited or no concern for calibration issues. In particular, the availability of accurate angular rate information might lead to more relaxed requirements as far as attitude sensors

Marco Bergamasco
Dipartimento di Elettronica e Informazione, Politecnico di Milano,
e-mail: bergamasco@elet.polimi.it

Marco Lovera
Dipartimento di Elettronica e Informazione, Politecnico di Milano e-mail: lovera@elet.polimi.it

are concerned, so it would be conceivable to operate the ACS loop using only static feedback from simple and low cost sensors such as magnetometers. Magnetometers have been used as reliable attitude sensors since the 1960s: as is well known (see, e.g., [17]), attitude information can be extracted from magnetometer measurements by comparing the sensed components of the geomagnetic field vector with a mathematical model of the field implemented on-board. Clearly, the accuracy of the obtained information will be affected both by measurement noise and by the accuracy of both the on-board field model and the knowledge of orbital position it requires as an input. Furthermore, on the basis of a single vector measurement such as the magnetic field it is not possible to get complete attitude information at each time instant, instead attitude observability is only guaranteed in an averaged sense. A classical approach to the design of a control law for this sensor configuration is to resort to a Kalman filter to reconstruct the missing attitude information (and possibly estimate gyro bias online) and close the loop using a conventional feedback based on the estimated states. While this approach is certainly the most appropriate one when dealing with the design of a high accuracy attitude controller for nominal operation, in many practical operating conditions it is desirable to be able to rely on much simpler controllers (i.e., static output feedback) while retaining a satisfactory level of pointing and stability performance near the nominal attitude.

In this paper (see also the preliminary results in [14]) the problem of deriving such a control law, i.e., a static output feedback one, with the aim of combining simplicity and reliability with an acceptable level of performance, is considered. More precisely, the above described sensor configuration consisting of a triaxial magnetometer (for attitude information) and three rate gyros is considered, a suitable pre-processing scheme for magnetometer measurements is proposed and the issues associated with the design of a static output feedback controller on the basis of such measurements are discussed. Simulation results are eventually used to illustrate the achievable performance in a realistic setting. From a design perspective, the main issue associated with this sensor configuration is that it leads to a linearised model with a time-periodic output equations, so that the design of the sought after output feedback controller calls for the adoption of methods and tools from the field of periodic systems and control (see [2]). More precisely, the method first presented in [15] has been employed.

The paper is organised as follows. In Section 2 a detailed model for the attitude dynamics of the considered spacecraft configuration is derived. Section 3 provides an overview of the adopted methods for control system design and compares an approach based on an approximate time-invariant model for the system with a more advanced one which takes into account periodicity of the output equation induced by the magnetometer model. Finally, in Section 4 some results obtained by applying the designed controller to a full nonlinear model of a LEO satellite are presented.

2 Mathematical model

2.1 Reference frames

In order to represent the attitude motion of an Earth-pointing spacecraft on a circular orbit the following reference systems are adopted:

- Earth Centered Inertial reference axes (ECI). The Earth's centre is the origin of these axes. The positive X-axis points in the vernal equinox direction. The Z-axis points in the direction of the North Pole. The Y-axis completes the right-handed orthogonal triad.
- Orbital Axes (X_O, Y_O, Z_O). The origin of these axes is at the satellite centre of mass. The X-axis points to the Earth's centre; the Y-axis points in the direction of the orbital velocity vector. The Z-axis is normal to the satellite orbit plane.
- Satellite Body Axes. The origin of these axes is at the satellite centre of mass; in nominal Earth- pointing conditions the X_B (yaw), Y_B (roll) and Z_B (pitch) axes are aligned with the corresponding orbital axes.

2.2 Attitude dynamics

For the purpose of the present study we consider as state variables the quaternion vector $q_{BO} = \left[q_r^T, q_4\right]^T \in \mathbf{R}^4$ representing the relative attitude of the satellite with respect to the orbital axes and the components $\omega_{BI} \in \mathbf{R}^3$ of the inertial angular rate vector of the satellite with respect to the body axes, so that

$$x = \begin{bmatrix} q_{BO} \\ \omega_{BI} \end{bmatrix}. \tag{1}$$

The state equations associated with the attitude dynamics are therefore given by (see, e.g., [13, 17])

$$\dot{x} = \begin{bmatrix} \frac{1}{2} W(\omega_{BO}) q_{BO} \\ I^{-1}(S(\omega_{BI}) I \omega_{BI} + T_g + T_c) \end{bmatrix}, \tag{2}$$

where $T_g \in \mathbf{R}^3$, $T_c \in \mathbf{R}^3$ are, respectively, the gravity-gradient and control torque vectors, the relative angular rate ω_{BO} is defined as

$$\omega_{BO} = \omega_{BI} - C_{BO}\omega_{OI} = \begin{bmatrix} \omega_x \\ \omega_y \\ \omega_z \end{bmatrix} - C_{BO} \begin{bmatrix} 0 \\ 0 \\ \Omega_{orb} \end{bmatrix}, \tag{3}$$

$C_{BO} \in \mathbf{R}^{3\times 3}$ being the attitude matrix corresponding to the quaternion q_{BO}, and

$$W(\omega_{BO}) = \begin{bmatrix} 0 & \omega_{BOz} & -\omega_{BOy} & \omega_{BOx} \\ -\omega_{BOz} & 0 & \omega_{BOx} & \omega_{BOy} \\ \omega_{BOy} & -\omega_{BOx} & 0 & \omega_{BOz} \\ -\omega_{BOx} & -\omega_{BOy} & -\omega_{BOz} & 0 \end{bmatrix}, \tag{4}$$

and

$$S(\omega_{BI}) = \begin{bmatrix} 0 & \omega_{BIz} & -\omega_{BIy} \\ -\omega_{BIz} & 0 & \omega_{BIx} \\ \omega_{BIy} & -\omega_{BIx} & 0 \end{bmatrix}. \tag{5}$$

With this choice of state variables we have that the quaternion, when the body system is coincident with the orbital system, is equal to the unit quaternion defined as $1_q = [0 \quad 0 \quad 0 \quad 1]^T$. The considered nominal state is therefore given by

$$x_{nom} = \left[1_q^T \ 0 \ 0 \ \Omega_{orb}\right]^T, \tag{6}$$

where Ω_{orb} is the orbital angular frequency.

2.3 Measurement models

As already discussed in the Introduction, the goal of this study is to demonstrate the feasibility of an attitude control design approach based solely on static feedback of magnetometer and gyro measurements. To this purpose, in this Section suitable models for such measurements will be defined.

2.3.1 Magnetometer measurement

The measurement provided by an (ideal) triaxial magnetometer can be simply defined as the vector of body-frame components of the geomagnetic field of the Earth. Therefore, letting b the onboard measured components of the Earth's magnetic field and b_O the Earth's magnetic field vector in orbital frame it holds that

$$b = C_{BO} b_O, \tag{7}$$

where C_{BR} is the attitude matrix from orbital frame to body frame. For the purpose of deriving an analytical expression of the linearised measurement model, the periodic dipole model for the geomagnetic field in orbital frame (see [9, 17]) can be considered, i.e.,

$$b_O(t) = \frac{\mu_F}{(R_E + a)^3} \begin{bmatrix} 2\sin(\Omega_{orb} t)\sin(i_m) \\ \cos(\Omega_{orb} t)\sin(i_m) \\ \cos(i_m) \end{bmatrix}, \tag{8}$$

where μ_F is the strength of the dipole of the Earth's magnetic field, i_m is the orbit's inclination with respect to the geomagnetic equator and R_E, a and Ω_{orb} are, respectively, the Earth radius, the orbit altitude and the orbit angular frequency. The simplified model of the magnetic field is considered reliable enough for control purposes, though the impact on stability and performance of the control system of the approximations implied by the use of such a simplified model have to be investigated a posteriori.

2.3.2 Gyro measurement

As far as gyros are concerned, in modelling the measurements available for control design it will be assumed that ideal access to the true components of the absolute angular rate is available. Again, the effect of measurement inaccuracies (see, again, [17]) will be taken into account in Section 4.

Remark 1. It is well known that the use of quaternion feedback for attitude control poses a number of conceptual and practical problems (see for example [1]). In the present work, however, no quaternion feedback is used in the control law; attitude information is fed back only via measurements of the geomagnetic field.

2.4 Linearised model

Since we are focusing on control law design for nominal operation, in the following, the linearised model describing the attitude motion near the nominal attitude is developed. As expected, the output equations associated with the selected measured variables turn out to be time periodic.

2.4.1 State equation

For the purpose of deriving a linearised version of the state equation (2), it will be assumed that $q_4 \simeq 1$, so that the state vector of the linearized model reduces to

$$\delta x = \begin{bmatrix} q_r \\ \omega \end{bmatrix} = \begin{bmatrix} 0_{5\times 1} \\ \Omega_{orb} \end{bmatrix} + \begin{bmatrix} \delta q_r \\ \delta \omega \end{bmatrix}. \tag{9}$$

In view of these definitions, the linearized model is given by

$$\begin{aligned} \delta \dot{x} &= \left.\frac{\partial F(x,u)}{\partial x}\right|_{Nom} \delta x + \left.\frac{\partial F(x,u)}{\partial u}\right|_{Nom} \delta u \\ &= \begin{bmatrix} \frac{\partial \dot{q}}{\partial q} & \frac{\partial \dot{q}}{\partial \omega} \\ \frac{\partial \dot{\omega}}{\partial q} & \frac{\partial \dot{\omega}}{\partial \omega} \end{bmatrix} \delta x + \begin{bmatrix} 0 \\ I^{-1} \end{bmatrix} \delta u, \end{aligned} \tag{10}$$

where

$$\frac{\partial \dot{q}}{\partial q} = \frac{1}{2}\frac{\partial}{\partial q} W(\omega_{BO}) q_{BO}\bigg|_{Nom} = \begin{bmatrix} 0 & \Omega_{orb} & 0 \\ -\Omega_{orb} & 0 & 0 \\ 0 & 0 & 0 \end{bmatrix}, \tag{11}$$

$$\frac{\partial \dot{q}}{\partial \omega} = \frac{1}{2}\frac{\partial}{\partial \omega} \left(W(\omega_{BO})\right)\bigg|_{Nom} = \frac{1}{2} I_3, \tag{12}$$

$$\frac{\partial \dot{\omega}}{\partial q} = \frac{\partial}{\partial q} I^{-1} T_g\bigg|_{Nom} = \tag{13}$$

$$= 6\Omega_{orb}^2 I^{-1} \begin{bmatrix} 0 & 0 & 0 \\ 0 & (I_{xx} - I_{zz}) & 0 \\ 0 & 0 & (I_{xx} - I_{yy}) \end{bmatrix}, \tag{14}$$

$$\frac{\partial \dot{\omega}}{\partial \omega} = \frac{\partial}{\partial \omega} I^{-1} S(\omega) I \omega\bigg|_{Nom} = \Omega_{orb} \begin{bmatrix} 0 & \frac{I_{yy} - I_{zz}}{I_{xx}} & 0 \\ \frac{I_{zz} - I_{xx}}{I_{yy}} & 0 & 0 \\ 0 & 0 & 0 \end{bmatrix}. \tag{15}$$

The expression $\frac{\partial \dot{\omega}}{\partial \omega}$ shown in (15) is valid only if the inertia matrix is diagonal, otherwise it assumes a more complex form. It is important to notice that subscripts are dropped in the following equations, but q and ω are the variables declared in the state vector (1). Substituting (11)-(15) in (10) the state equation of the linearized model is obtained.

2.4.2 Output equation

Linearising (7) one gets

$$b \simeq b_O + 2S^T(b_O)\delta q, \tag{16}$$

where

$$S(b_O) = \begin{bmatrix} 0 & b_{Oz} & -b_{Oy} \\ -b_{Oz} & 0 & b_{Ox} \\ b_{Oy} & -b_{Ox} & 0 \end{bmatrix}. \tag{17}$$

In view of the problem of designing a static output feedback controller, it is useful to modify the output equation so as to get a (time-varying) gain between the linearised vector part of the quaternion and the output which is: i) positive semidefinite and ii) as close as possible to an identity matrix. This can be achieved by defining the output associated with magnetometer measurements as

$$y_1 = \frac{1}{2\|b_O\|^2} S(b_O) b \simeq \frac{1}{\|b_O\|^2} S(b_O) S^T(b_O) \delta q. \tag{18}$$

For the angular rate measurements one can simply define the output as $y_2 = \omega$, so the overall output equation for the linearised model reads

$$\delta y = \begin{bmatrix} \delta y_1 \\ \delta y_2 \end{bmatrix} = C(t)\delta x = \begin{bmatrix} \frac{1}{\|b_O\|^2} S(b_O) S^T(b_O) \\ I_3 \end{bmatrix} \begin{bmatrix} \delta q \\ \delta \omega \end{bmatrix}. \tag{19}$$

As is well known from the literature (see, e.g., [16]), if full attitude and angular rate feedback were available (i.e., if we were to replace the periodic matrix gain $\frac{1}{\|b_O\|^2} S(b_O) S^T(b_O)$ with an identity matrix) then local closed loop stability would be guaranteed for any positive value of the proportional and derivative controller gains. In the case of attitude feedback provided by a magnetometer, however, closed loop stability may be significantly affected by the choice of such parameters. This is due to the fact that feedback from the magnetometers renders the closed loop dynamics time-periodic, so that stability of the closed loop system depends on the controller parameters in a fundamentally different way. In particular, this implies that analysis and design have to be carried out using tools from periodic systems theory, as will be discussed in detail in the following Section.

3 Controller design

3.1 Design approach

In this Section, an overview of the approach to the design of LQ-optimal constant gain controllers for continuous-time LTP systems, first presented in [15], will be provided. Consider the LTP system

$$\begin{aligned} \dot{x}(t) &= A(t)x(t) + B(t)u(t) \\ y(t) &= C(t)x(t) \end{aligned} \tag{20}$$

where $A(t) \in \mathbf{R}^{n\times n}, B(t) \in \mathbf{R}^{n\times m}, C(t) \in \mathbf{R}^{p\times n}$ are T-periodic matrices, and the quadratic performance index

$$J = E\left\{ \int_{t_0}^{\infty} \left[x^T(t)Q(t)x(t) + u^T(t)R(t)u(t) \right] dt \right\} \tag{21}$$

with $Q(t) = Q^T(t) \geq 0, R(t) = R^T(t) > 0$ T-periodic matrices and where the expectation is taken over the initial condition x_0, modelled as a random variable with zero mean and known covariance $X_0 = E\left\{x_0 x_0^T\right\}$. The optimal output feedback control problem can be formulated as follows: find the constant feedback matrix F of optimal control action

$$u^*(t) = Fy(t) \tag{22}$$

which minimizes the performance index J of (21). Holding (22), the closed loop dynamics can be written as

$$\dot{x} = [A(t) + B(t)FC(t)]\,x = \bar{A}(t)x \tag{23}$$

where $\bar{A}(t) = A(t) + B(t)FC(t)$ represents the closed loop dynamic matrix, which is obviously periodic. Therefore matrix $\bar{A}(t)$ is associated with the transition matrix $\Phi_{\bar{A}}(t,t_0)$ satisfying

$$\dot{\Phi}_{\bar{A}}(t,t_0) = \bar{A}(t)\Phi_{\bar{A}}(t,t_0), \;\; \Phi_{\bar{A}}(t_0,t_0) = I_n. \tag{24}$$

The minimization of the performance index given by (21) can be carried out using either gradient-free or gradient-based methods, provided that an analytical expression for the gradient of the performance index with respect to the F matrix is available. In both cases, an initial stabilizing matrix F_0 must be employed. In the following Proposition (see [15] for details), necessary conditions for optimality (and therefore the required gradient expression) will be presented.

Proposition 1 *Let F be a constant stabilizing output feedback gain and assume that the matrices $\bar{A}(t)$, $\bar{Q}(t)$ and $X(t)$ are given respectively by $\bar{A} = A + BFC$, $\bar{Q} = Q + C^T F^T RFC$ and $X(t) = \Phi_{\bar{A}}(t,t_0)X_0\Phi_{\bar{A}}^T(t,t_0)$; hence, the expressions for the performance index* (21) *and its gradient are given by*

$$J(F,X_0) = trace\,(P_0X_0)$$

$$\nabla_F J(F,X_0) = 2\int_{t_0}^{t_0+T} \left[B^T(t)P(t) + \right. \\ \left. + R(t)FC(t)\right]\Phi_{\bar{A}}(t,t_0)V\Phi_{\bar{A}}^T(t,t_0)C^T(t)dt$$

where the symmetric periodic matrices $P(t)$ and V satisfy, respectively, the periodic Lyapunov differential equation (PLDE)

$$-\dot{P}(t) = \bar{A}^T(t)P(t) + P(t)\bar{A}(t) + \bar{Q}(t)$$

and the discrete Lyapunov equation (DLE)

$$V = \Psi V \Psi^T + X_0.$$

The optimization of (21) requires that the LTP system (20) is output stabilizable and, at each iteration i, the matrix F_i belongs to the set $\mathscr{S}_F \subset \mathbf{R}^{m\times p}$ of the stabilizing feedback gain matrices. Formally, the optimization problem can be stated as

$$\min_{F\in\mathscr{S}_F} J(F,X_0). \tag{25}$$

The stopping criterion, indicating convergence to a global or, at least, a local solution of (25) will be simply $\|\nabla_F J\| < tol$.

Remark 2. Feasibility is a critical issue in the design of static output feedback. For the problem at hand, however, it can be easily shown that the average of matrix $C(t)$ in (19) over one orbit period is nonsingular, so that the considered static output feedback problem is equivalent (in the sense of averaging theory, see [7]) to a state feedback one and is, therefore, feasible.

3.2 Controller design

The above described design approach has been applied to the linearised model derived in Section 2, with specific reference to the case study described in the following Section 4.2. More precisely, as far as the LQP design approach is concerned, the weighting matrices in (21) have been chosen as $Q = I_6$ and $R = 10^3 I_3$; the computed output-feedback gain leads to a stable closed-loop system, with the following values for the characteristic multipliers (see [2])

$$\lambda_{LQP} = \left[0.0339\ 0.0000\ 0.0000\ 0\ 0\ 0\right]. \tag{26}$$

In order to be able to quantify the benefits of taking the periodicity of the linearised model into account in the design of the control law, a second controller has been designed using a time-invariant approximation of the linearised model obtained by computing the average over one orbit period $T = 2\pi/\Omega_{orb}$ of matrix $C(t)$ in (19)

$$\bar{C} = \frac{1}{T}\int_0^T C(t)dt. \tag{27}$$

As $\bar{C}$ turns out to be nonsingular, for the averaged linearised model it is possible to design a constant gain controller by solving a state feedback rather than an output feedback problem. The control law is given by

$$\delta u = F\delta y, \tag{28}$$

with $F = -K\bar{C}^{-1}$, where K is the LQ state-feedback gain computed using the same Q and R weighting matrices as in the periodic design case. In order to check the closed-loop stability of the original linearised periodic system under the feedback (28), the characteristic multipliers of the closed-loop system have been computed:

$$\lambda_{LQ} = \left[0.5369\ 0.0673\ 0.0003\ 0\ 0\ 0\right]. \tag{29}$$

The linearized model and the gains computed with the two design approaches have been implemented and the performance of these control laws have been assessed. In the simulations, the initial state

$$x_0 = \left[0.05\ 0.05\ 0.05\ 0.001\ 0.001\ 0.001\right]^T, \tag{30}$$

has been considered, which corresponds to an error of about 5.7° between the body frame and the orbital frame for each axis and to an error close to Ω_{Orb} on the body components of the angular rate, i.e., a representative initial condition for a nominal attitude controller.

The results of the simulations are shown in Figures 1-3. As can be seen, both control laws bring the satellite back to its nominal attitude, removing the initial attitude and angular rate error by applying control torques of acceptable values. A

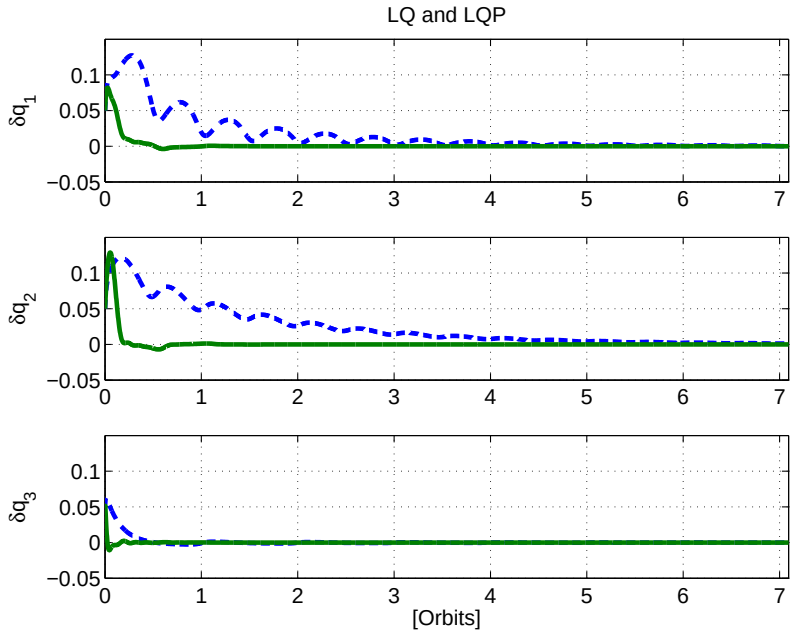

Fig. 1: Closed-loop time histories of δq_r using the LQ (dashed lines) and LQP (solid lines) controllers.

comparison of the closed-loop dynamics obtained using the two controllers, however, show clearly that using the design approach capable of taking the periodicity of the output equation into account a better result can be obtained, namely a faster and smoother transient for the attitude parameters. Indeed, with similar control torques the LQ controller brings the satellite in nominal attitude in about 5 orbits ($\approx$ 30000 s), while the LQP controller achieves the same results much more effectively, i.e., in less than one orbit. The above comparison, however, has been performed in a rather ideal setting, i.e., by simulating the linearised model for the attitude dynamics and neglecting all the sources of uncertainty which have been mentioned in Section 2. A more realistic simulation study is presented in the following Section.

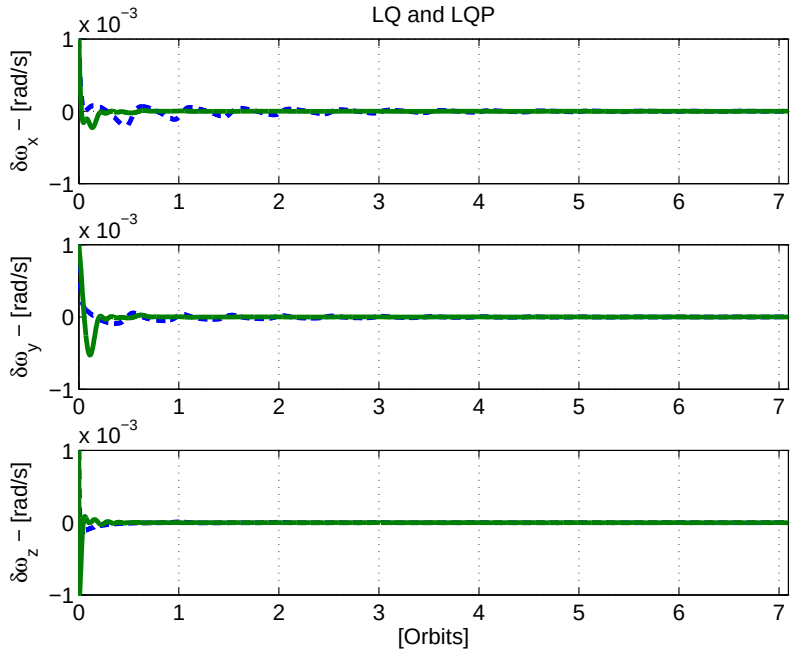

Fig. 2: Closed-loop time histories of $\delta\omega$ using the LQ (dashed lines) and LQP (solid lines) controllers.

4 Simulation study

In order to assess the achievable performance using the magnetometer+gyros configuration and the proposed design approach, a more realistic simulation study has been performed. In this Section, the simulation environment, the considered case study and the obtained results are presented and discussed.

4.1 Simulation environment

The simulations presented in the following have been carried out using an object-oriented environment for satellite dynamics (see [8, 12] for details) developed using the Modelica language ([5]). More precisely, a full nonlinear simulation of the coupled rigid body orbital and attitude dynamics has been performed and the following models of the space environment have been implemented: the *JGM*-3 spherical expansion for the geopotential as a gravitational model, the Harris-Priester model for the atmospheric density distribution (see [10] for details) and the International Ge-

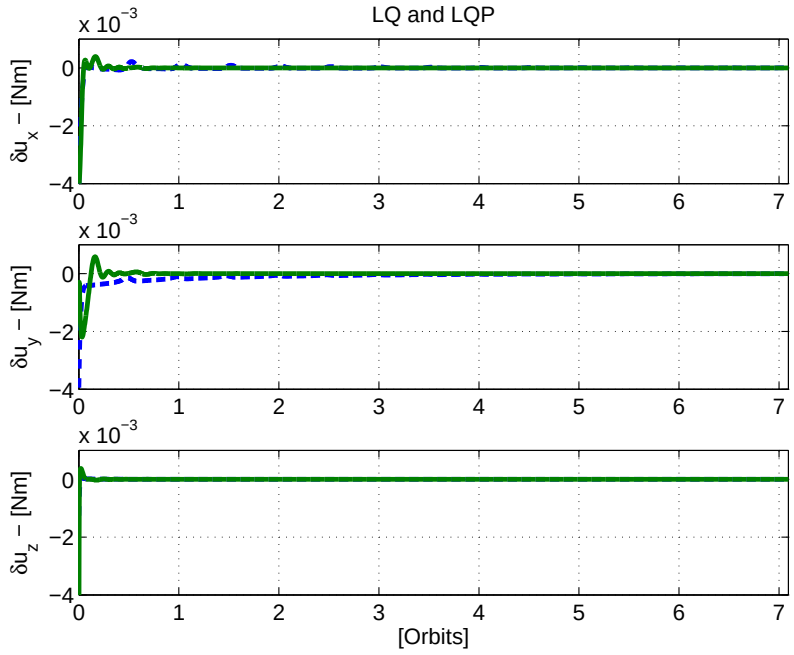

Fig. 3: Control torques, using the LQ (dashed lines) and LQP (solid lines) controllers.

omagnetic Reference Field (IGRF, see [17]) for the Earth's magnetic field (up to order 10). Disturbance torques due to gravity gradient (including J_2 effects), magnetic residual dipole (assuming a residual dipole of 1 $\mathrm{A\,m^2}$ along each spacecraft body axis) and solar radiation pressure (computed using the solar coordinates formulas given in [10]) have been taken into account in the simulation. Finally, the controller has been implemented in digital form, using a conventional sample and hold scheme and a sampling interval of one second.

4.2 Case study

The considered case study is loosely based on the spacecraft for the ESA Swarm mission (see [6]), the goal of which is to provide the best ever survey of the geomagnetic field and the first global representation of its variation on time scales from an hour to several days. The Swarm concept consists of a constellation of three satellites in three different polar orbits between 400 and 550 km altitude. For the purpose of this study the following assumptions have been made:

1. The satellite is operating on a circular, near polar orbit ($i = 86.9^\circ$ inclination) with an altitude of 450 km (and a corresponding orbital period of 5614.8 seconds).
2. The satellite inertial properties are:
   - Satellite mass $m = 496$ [kg]
   - Satellite inertia matrix:

$$I = \begin{bmatrix} 465.8 & -15 & -1 \\ -15 & 48.5 & -2.8 \\ -1 & -2.8 & 439.9 \end{bmatrix} \quad [\text{kg m}^2]. \tag{31}$$

3. For aerodynamic modelling purposes, a default cubic geometry was assumed for the satellite, comprising six surfaces, each with 1 m^2 surface area, reflectivity coefficient $\varepsilon = 0.02$ and center of pressure located at the surface geometric center. As far as the interaction with the environment is concerned, aerodynamic drag, solar radiation pressure and a residual magnetic dipole of 1 A m^2 upon each spacecraft body axis were considered as sources of disturbance torques.
4. Representative values for the errors affecting sensor measurements (magnetometer, gyros, GPS data) have been taken into account.

Finally, as mentioned in Section 2 an important factor which influences the reliability of geomagnetic field measurements as sources of attitude information is the accuracy of the on-board geomagnetic field model to which the measurements are compared. In order to evaluate the sensitivity of the closed-loop performance in this respect, the controller designed in the previous Section has been implemented and used in closed-loop simulations both by assuming the on-board availability of a very accurate geomagnetic field model (10th order IGRF model, i.e., same order as the "truth" model) and by considering a less precise one (5th order IGRF only).

4.3 Simulation results

The results obtained in the simulations are presented in Figures 4-6. As can be seen, the controller designed using the proposed approach can provide excellent performance in terms of transient response even in this more realistic scenario, i.e., taking into account disturbance torques, measurement and modelling errors and the digital implementation. Furthermore, while the performance degradation associated with geomagnetic field modelling errors is clearly visible in Figures 4-5, the overall pointing accuracy is satisfactory.

5 Conclusions

In this paper, the problem of attitude control system design for a Low Earth Orbit (LEO) satellite equipped with a triaxial magnetometer and a set of high preci-

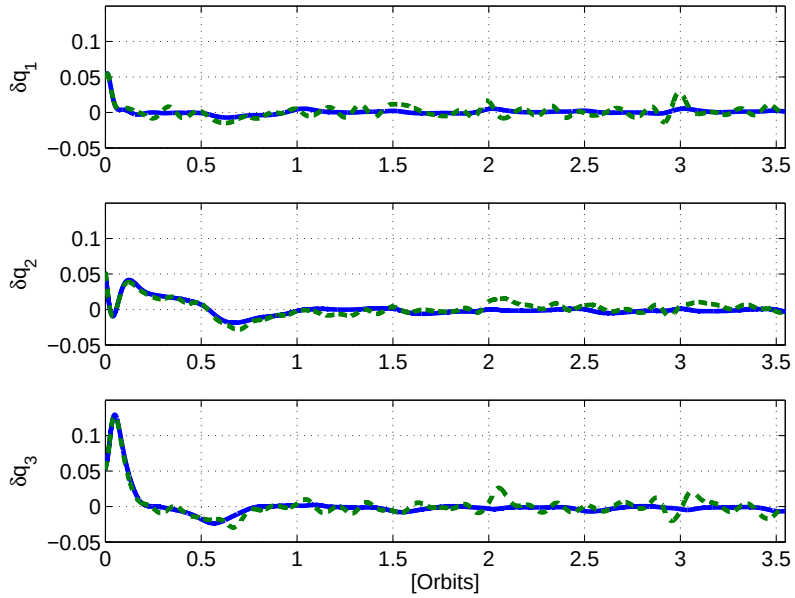

Fig. 4: Closed-loop time histories of δq_r using the 5th order (dashed lines) and the 10th order (solid lines) IGRF magnetic field model on-board.

sion gyros has been considered. This sensor configuration leads to a time-periodic linearised model, for the control of which an approach based on optimal static output feedback for linear time-periodic system has been presented. Simulation results have been used to demonstrate the practical feasibility of the proposed strategy and to quantify the achievable performance in a realistic setting for a LEO satellite mission.

References

1. S.P. Bhat and D. Bernstein. A topological obstruction to continuous global stabilization of rotational motion and the unwinding phenomenon. *Systems & Control Letters*, 39(1):63–70, 2000.
2. S. Bittanti and P. Colaneri. *Periodic Systems: Filtering and Control*. Springer, 2008.
3. A. Cropp, C. Collingwood, and S. Dussy. The Characterisation and Testing of MEMS Gyros for GIOVE-A. In *AIAA Guidance, Navigation, and Control Conference and Exhibit, Keystone, Colorado*, number AIAA 2006-6044, 2006.
4. J. Ford and M. Evans. Online estimation of Allan variance parameters. *Journal of Guidance, Control and Dynamics*, 23(6):980–987, 2000.
5. P. Fritzson and Bunus. Modelica - a general object-oriented language for continuous and discrete-event system modelling and simulation. In *Proceedings of the 35th IEEE Annual Simulation Symposium*, 2002.

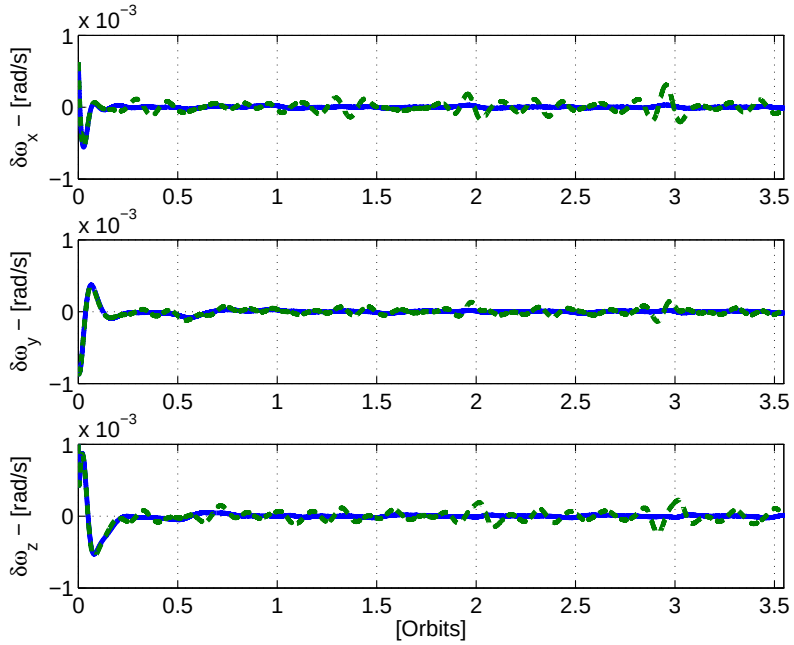

Fig. 5: Closed-loop time histories of $\delta\omega$ using the 5th order (dashed lines) and the 10th order (solid lines) IGRF magnetic field model on-board.

6. R. Haagmans. Swarm - the earth's magnetic field and environment explorers. Technical Report SP-1279(6), ESA, 2004.
7. H.K. Khalil. *Nonlinear systems*. Macmillan, 1992.
8. M. Lovera. Control-oriented modelling and simulation of spacecraft attitude and orbit dynamics. *Journal of Mathematical and Computer Modelling of Dynamical Systems, Special issue on Modular Physical Modelling*, 12(1):73–88, 2006.
9. M. Lovera and A. Astolfi. Global magnetic attitude control of spacecraft in the presence of gravity gradient. *IEEE Transactions on Aerospace and Electronic Systems*, 42(3):796–805, 2006.
10. O. Montenbruck and E. Gill. *Satellite orbits: models, methods, applications*. Springer, 2000.
11. C. Pearce. The performance and future development of a MEMS SiVSG and its application to the SiIMU. In *AIAA Guidance, Navigation, and Control Conference and Exhibit, Montreal, Canada*, number AIAA 2001-4410, 2001.
12. T. Pulecchi. *Advanced Techniques for Satellite Modeling and Attitude Control*. PhD thesis, Politecnico di Milano, 2008.
13. M. Sidi. *Spacecraft dynamics and control*. Cambridge University Press, 1997.
14. L. Viganó, M. Bergamasco, M. Lovera, and A. Varga. Optimal periodic output feedback control: a continuous-time approach and a case study. *International Journal of Control*, 83(5):897–914, 2010.
15. L. Vigano', M. Lovera, and A. Varga. Optimal periodic output feedback control: a continuous time approach. In *3rd IFAC Workshop on Periodic Control Systems, Saint Petersburg, Russia*, 2007.
16. J. T.-Y. Wen and K. Kreutz-Delgado. The attitude control problem. *IEEE Transactions on Automatic Control*, 36(10):1148–1162, 1991.

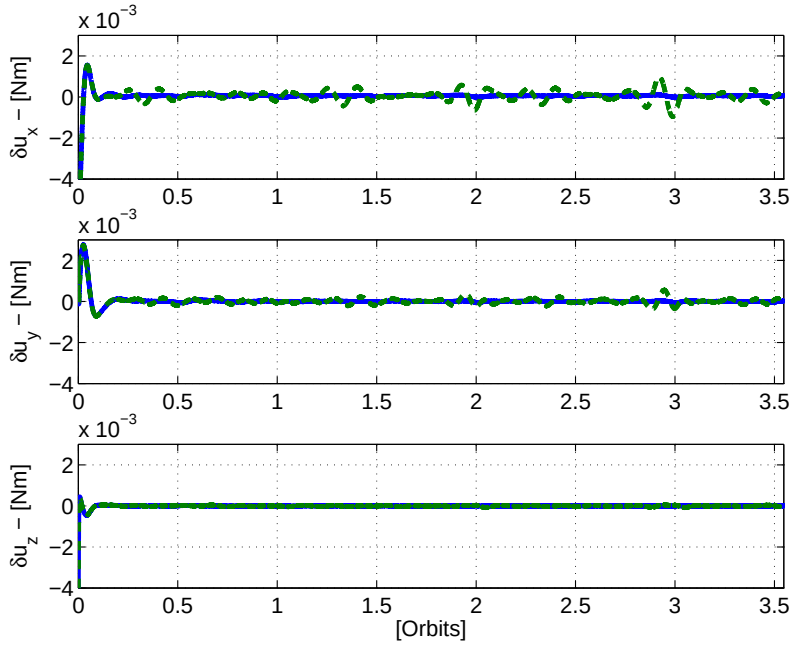

Fig. 6: Control torques, using the 5th order (dashed lines) and the 10th order (solid lines) IGRF magnetic field model on-board.

17. J. Wertz. *Spacecraft attitude determination and control*. D. Reidel Publishing Company, 1978.